

FAST RADIO BURSTS FROM THE COLLAPSE OF STRANGE STAR CRUSTS

YUE ZHANG¹, JIN-JUN GENG^{1,2}, AND YONG-FENG HUANG^{1,2}

¹School of Astronomy and Space Science, Nanjing University, Nanjing 210023, China

²Key Laboratory of Modern Astronomy and Astrophysics (Nanjing University), Ministry of Education, China

ABSTRACT

Fast radio bursts (FRBs) are transient radio sources at cosmological distances. No counterparts in other bands have been observed for non-repeating FRBs. Here we suggest the collapse of strange star crusts as a possible origin for FRBs. Strange stars, which are composed of almost equal numbers of u, d, and s quarks, may be encapsulated by a thin crust of normal hadronic matter. When a strange star accretes matter from its environment, the crust becomes heavier and heavier. It may finally collapse, leading to the release of a large amount of magnetic energy and plenty of electron/positron pairs on a very short timescale. Electron/positron pairs in the polar cap region of the strange star can be accelerated to relativistic velocities, streaming along the magnetic field lines to form a thin shell. FRBs are produced by coherent emission from these electrons when the shell is expanding. Basic characteristics of observed FRBs can be explained in our model.

Keywords: radiation mechanisms: non-thermal – radio continuum: general – stars: neutron

1. INTRODUCTION

Fast radio bursts (FRBs) are a new kind of phenomena that were discovered in the past decade [Lorimer et al. \(2007\)](#); [Thornton et al. \(2013\)](#); [Keane et al. \(2012\)](#). These transient bursts have flux densities of $S_\nu \sim$ a few Jy at frequencies of $\nu_{\text{FRB}} \sim 1$ GHz, with the waveband width of $\Delta\nu_{\text{FRB}} \sim$ several hundred MHz. Their durations δt are typically a few ms, indicating a rather compact region of emission. The observed high dispersion measurements (DMs) of $\sim 500 - 1000$ pc cm⁻³ are well above the contribution from our Galaxy for several FRBs detected at high-galactic-latitude ($\geq 40^\circ$) [Cordes & Lazio \(2002\)](#); [Luan & Goldreich \(2014\)](#), suggesting that the sources are at cosmological distances of $d \sim$ Gpc with redshifts of $z \sim 0.5 - 1$. Hence the isotropic luminosities in radio waves (L_{FRB}) are estimated as $\sim 10^{42} - 10^{43}$ erg s⁻¹, with the total isotropic energy released in a typical burst being $E_{\text{FRB}} \sim 10^{39} - 10^{40}$ erg. The event rate is estimated to be $\sim 2 \times 10^3$ sky⁻¹ day⁻¹ [Bhandari et al. \(2018\)](#). The brightness temperatures of FRB sources can be as high as $T_B \geq 10^{36}$ K [Luan & Goldreich \(2014\)](#); [Katz \(2014\)](#), where Γ is the Lorentz factor of the emitting material. Such an extremely high temperature is far above the Compton limit for incoherent synchrotron radiation, thus a coherent origin shall be considered [Romero et al. \(2016\)](#). On the other hand, no counterparts in other wavebands have been detected to associated with non-repeating FRBs hitherto.

The origin of FRBs still remains unclear, but a number of models trying to interpret these enigma phenomena have been proposed, e.g., magnetar giant flares [Kulkarni et al. \(2014\)](#), the collapses of magnetized supramassive rotating neutron stars [Falcke & Rezzolla \(2014\)](#); [Zhang \(2014\)](#), binary neutron star mergers [Totani \(2013\)](#), binary white dwarf mergers [Kashiyama et al. \(2013\)](#), collisions between neutron stars and asteroids/comets [Geng & Huang \(2015\)](#), collisions between neutron stars and white dwarfs [Liu \(2017\)](#), and evaporation of primordial black holes [Barrau et al. \(2014\)](#). Some of these models are catastrophic and the original central engines are destroyed completely by the bursts. The discovery of the repeating FRB source, i.e., FRB 121102 [Spitler et al. \(2016\)](#); [Scholz et al. \(2016\)](#), presents new interesting clues to FRBs. Several elaborate models have been put forward to explain its repeating behaviors, e.g., highly magnetized pulsars traveling through asteroid belts [Dai et al. \(2016\)](#), neutron star-white dwarf binary mass transfer [Gu et al. \(2016\)](#), and star quakes of pulsars [Wang et al. \(2018\)](#). However, it is wondered whether FRB 121102 is representative of FRBs since its features are different from others [Palaniswamy et al. \(2018\)](#); [Michilli et al. \(2018\)](#). Naturally, people speculate that repeating FRBs such as FRB 121102 may be a separate kind of FRB sources.

Here we propose a new model for FRBs. We argue that the collapse of strange star (SS) crusts can also explain the main features of FRBs. The structure of this paper is as follows. In Section 2, the process of SS crust collapse is illustrated. The emission mechanism that leads to observable FRBs is described in Section 3. Possible counterparts

in other wavebands are discussed in Section 4. Finally, Section 5 is a brief summary and discussion.

2. COLLAPSE PROCESS OF SS CRUST

It has been conjectured that strange quark matter (SQM), a kind of dense material composed of approximately equal numbers of up, down, and strange quarks, may have a lower energy per baryon than ordinary nuclear matter (such as ^{56}Fe) so that it may be the true ground state of hadronic matter [Witten \(1984\)](#); [Abe et al. \(1984\)](#). If this hypothesis is correct, then neutron stars (NSs) may actually be “strange stars” [Alcock et al. \(1986\)](#). The bulk properties of strange stars and neutron stars are rather similar in the typical mass range of $1 \leq M/M_\odot \leq 1.8$, and it is very difficult to discriminate between them [Haensel et al. \(1986\)](#). Although several methods have been proposed to distinguish strange stars from neutron stars [Geng et al. \(2015\)](#); [Lai et al. \(2018\)](#), no definitive conclusions have been drawn yet.

At the strange star SQM surface, the density reduces from $\sim 5 \times 10^{14} \text{ g cm}^{-3}$ to zero abruptly. The thickness of the SQM surface is of order 1 fm due to strong interaction between quarks, while electrons can stretch up to several hundred fm beyond the surface since they are bounded electromagnetically. An extremely intense electric field ($\sim 5 \times 10^{17} \text{ V/cm}$) is induced by charge separation near the SQM surface [Alcock et al. \(1986\)](#). The outward-directed electric field can polarize a layer of nearby normal matter and provide a force overwhelming the gravity [Huang & Lu \(1997\)](#); [Stejner & Madsen \(2005\)](#). As a result, a thin crust composed of normal hadronic matter may exist and obscure the whole surface of the SQM core. It has been shown by [Huang & Lu \(1997\)](#) that the maximum density at the bottom of the crust should be significantly less than the so called neutron drip density. For a typical SS with a radius of $r \sim 10 \text{ km}$, a mass of $M \sim 1.4 M_\odot$ and a surface temperature of $T_s \sim 3 \times 10^7 \text{ K}$, the crust mass is usually in the range of $M_c \sim 10^{-7} M_\odot - 10^{-5} M_\odot$ and its thickness is about $l \sim 2 \times 10^4 \text{ cm}$.

The distance between the bottom of the crust and the surface of the SQM core shall be at least $\sim 200 \text{ fm}$ so that the rate at which ions penetrate the gap through the tunneling effect is low enough to ensure the stabilization of the crust [Alcock et al. \(1986\)](#). If the mass of the crust increases continuously via some accreting process, then the gap between the crust bottom and the SQM surface will become narrower and narrower to counterpoise the gravity of the crust [Huang & Lu \(1997\)](#). Once the gap is less than $\sim 200 \text{ fm}$, a large portion of ions could penetrate the Coulomb barrier and reach the SQM core. They will be converted to SQM and the surface of the SQM core will be heated, which further reduces the electric field and hence the gap width [Kettner et al. \(1995\)](#). Consequently, a faster tunneling penetration is stimulated by the decreased gap width. This is a positive feedback and the SS crust will finally collapse completely on a free-fall timescale of $\sim 0.1 \text{ ms}$.

Although the detailed mechanism for maintaining a strong magnetic field in various compact stars is still largely uncertain, it is believed that SSs can also have a strong magnetic field. When the crust of an SS breaks and falls into the SQM core, the magnetic field lines in the crust will be dragged into the core due to Alfvén’s frozen effect. A fraction of the magnetic energy originally embedded in the crust will be transferred to radiation. In fact, after the collapse of the SS crust, the magnetic field lines near the polar cap region will be disturbed and twisted because of differential rotation and/or magnetic instabilities [Kashiyama et al. \(2013\)](#). Hence transient dissipation processes such as magnetic reconnection may be triggered [Thompson & Duncan \(1995\)](#), and the magnetic energy will be released on a short timescale.

Theoretically, the limiting interior magnetic field is of the order of $B_{\text{max}} \sim 10^{18} M_1 r_6^{-2} \text{ G}$, where the SS is assumed to have a mass of $M = M_1 M_\odot$ and a radius of $r = r_6 10^6 \text{ cm}$ [Lai & Shapiro \(1991\)](#). The convention $Q_x = Q/10^x$ in cgs units is adopted hereafter. Pulsars with surface magnetic fields up to $\sim 10^{14} \text{ G}$ have been reported, and there is no “smoking-gun” evidence to identify them as neutron stars or SSs [Kouveliotou et al. \(1998\)](#). It is reasonable to postulate that some SSs could have a surface magnetic field as strong as $B_s \sim 10^{14} \text{ G}$ in the polar cap region, where the field should be the strongest for a dipole configuration. A dipole field approximation $B(R) \approx B_s \times (R/r)^{-3}$ is applied in our paper, where R is the distance from the SS center. The total magnetic energy stored in the crust can be expressed as $E_B \sim 4\pi r^2 l \times B_s^2/8\pi \sim 5 \times 10^{43} B_{s,14}^2 r_6^2 l_4 \text{ erg}$.

In our framework, we believe that an FRB is produced mainly from the polar cap region, so not all the E_B energy is available for generating the FRB. The angular size of the polar-cap region is approximately $\theta_{\text{cap}} \sim 1.45 \times 10^{-2} P_0^{-1/2} r_6^{1/2}$, where P is the rotation period of the SS. The magnetic energy included in the polar region can then be estimated as $E_{B,\text{cap}} \sim E_B \times \pi \theta_{\text{cap}}^2/4\pi \sim 2.6 \times 10^{39} P_0^{-1} B_{s,14}^2 r_6^3 l_4 \text{ erg}$. We suppose that the radio emission is restricted in an area with the solid angle of $4\pi f$, where f is a parameter characterizing the beaming fraction. The energy needed to produce an FRB is then $\sim f E_{\text{FRB}}$, where E_{FRB} is the isotropic FRB energy. Assuming η to be the fraction of $E_{B,\text{cap}}$ that is emitted, it can be calculated as $\eta \sim f E_{\text{FRB}}/E_{B,\text{cap}} \sim 0.4 f P_0 B_{s,14}^{-2} r_6^{-3} l_4$. If we take $f \sim 0.1$ and $P \sim 1 \text{ s}$ [Kondratyuk et al. \(1990\)](#), η can be reckoned as ~ 0.04 .

In short, as long as a small fraction of the magnetic energy conserved in SS polar cap regions is transferred into

radiation during the collapse process, the energy is adequate for an FRB. FRBs should be connected with coherent emission mechanism for their extremely high brightness temperature [Katz \(2014\)](#). We will discuss the detailed radiation process below.

3. EMISSION MECHANISM

After the crust collapse, the SS becomes hot and bare. It turns into a powerful source of electrons and positrons (e^+e^-) pairs. These e^+e^- pairs are created in an extremely strong electric field [Usov \(1998a\)](#). Near the polar cap region where the magnetic field energy is released, electrons and positrons will be accelerated to ultra-relativistic speeds [Ruderman & Sutherland \(1975\)](#); [Benford & Buschauer \(1977\)](#). These particles coast along the magnetic field lines and form a shell with a thickness of $\delta r_{\text{emi}} \approx c\delta t$. This process is illustrated in Figure 1.

Curvature radiation will be produced when electrons in the shell are streaming along parallel magnetic field lines. For simplicity, we postulate that all electrons are moving with almost exactly the same velocity (i.e., with the corresponding Lorentz factor of γ), and δr_{emi} remains roughly constant in the observer frame as long as $\delta r_{\text{emi}} > \gamma^{-2}r_{\text{emi}}$ like the fireballs in the cases of gamma-ray bursts [Rees & Mészáros \(1992\)](#). Let r_{emi} be the emission radius of the shell and r_c be the curvature radius of the magnetic field lines, then the shell volume is $V_{\text{emi}} \approx 4\pi f r_{\text{emi}}^2 \delta r_{\text{emi}}$. The patch in which electrons radiate coherently has a characteristic radial size $\lambda \approx c/\nu_c$ and a solid angle $4/\gamma^2$ according to beaming effects. Such a patch has a volume of $V_{\text{coh}} \approx (c/\nu_c) \times (4/\gamma^2)r_{\text{emi}}^2$ [Kumar et al. \(2017\)](#); [Kashiyama et al. \(2013\)](#). In the emission region, there are $N_{\text{pat}} \approx V_{\text{emi}}/V_{\text{coh}}$ coherent patches totally, and each patch has $N_{\text{coh}} \approx n_e \times V_{\text{coh}}$ electrons in it, where n_e is the electron number density. The frequency of curvature emission is $\nu_c \approx \gamma^3(3c/4\pi r_c) \approx \nu_{\text{FRB}}$. The total coherent curvature emission luminosity from these electrons can be expressed as $L_{\text{total}} \approx (P_e N_{\text{coh}}^2) \times N_{\text{pat}}$, where $P_e = 2\gamma^4 e^2 c / 3r_c^2$ is the emission power of a single electron [Kashiyama et al. \(2013\)](#).

According to [Benford & Buschauer \(1977\)](#), the coherent radiation peaks at the places where the relativistic plasma energy density just exceeds the dipolar field energy density. With the plasma pressure of $\rho_P(R) \approx n_e \gamma m_e c^2$, the magnetic energy density of $\rho_M(R) \approx B^2(R)/8\pi$, and assuming $r_{\text{emi}} \sim r_c$, the emission radius can be estimated as

$$r_{\text{emi}} \sim 0.6 \times 10^{10} \left(f_{-1}^3 L_{\text{total},43}^{-3} \delta t_{-3}^3 \nu_{\text{FRB},9}^{-1} B_{\text{S},14}^{12} r_{c,10}^{36} \right)^{1/25} \text{ cm}. \quad (1)$$

On other hand, the electron Lorentz factor γ can be derived as

$$\gamma \sim 1120 \nu_{\text{FRB},9}^{1/3} r_{c,10}^{1/3}. \quad (2)$$

The total coherent curvature emission luminosity from these electrons can be expressed as [Kashiyama et al. \(2013\)](#)

$$\begin{aligned} L_{\text{total}} &\approx (P_e N_{\text{coh}}^2) \times N_{\text{pat}} \\ &\sim 2.6 \times 10^{42} \text{ erg s}^{-1} \\ &\times f n_{e,7}^2 \delta t_{-3}^{-1/3} \nu_{\text{FRB},9}^{-1/3} r_{\text{emi},10}^4 r_{c,10}^{-4/3}. \end{aligned} \quad (3)$$

Then the observed isotropic FRB luminosity $L_{\text{FRB}} \approx f^{-1} L_{\text{total}} \sim 10^{42-43} \text{ erg s}^{-1}$ is consistent with observations.

The typical emission frequency should be larger than the plasma characteristic frequency so that the radio waves can propagate without being absorbed [Benford & Buschauer \(1977\)](#); [Kashiyama et al. \(2013\)](#), i.e.,

$$\nu_{\text{FRB}} > f_{\text{pe}} \approx \left(\frac{\gamma n_e e^2}{\pi m_e} \right)^{1/2}. \quad (4)$$

It requires that

$$n_e \leq 1.1 \times 10^7 \nu_{\text{FRB},9}^{5/3} r_{c,10}^{-1/3} \text{ cm}^{-3}. \quad (5)$$

Another requirement is that the induced Compton scattering should not be too strong to hinder the propagation of the radio wave in the plasma [Melrose \(1971\)](#). The Lorentz factor of the relativistic plasma is therefore limited by (see Equation (53) of [Lyubarsky \(2008\)](#))

$$\begin{aligned} \gamma &> 730 \gamma_T^{-1/4} \zeta^{-1/8} \nu_{\text{FRB},9}^{-1/8} \\ &\times \left(\frac{F}{1 \text{ Jy}} \right)^{1/4} \left(\frac{\delta t}{5 \text{ ms}} \right)^{-3/8} \left(\frac{D}{100 \text{ Mpc}} \right)^{1/2}. \end{aligned} \quad (6)$$

Here $\gamma_T \sim 1$ is the thermal Lorentz factor of the electrons/positrons in the plasma's co-moving frame, ζ is the fraction of the plasma energy radiated in radio, F is the radio flux density, and D is the distance to the source. Comparing Equation (6) with Equation (2), we find that this requirement can be reasonably satisfied.

The coherent energy loss rate per electron is $P_e N_{\text{coh}} \sim 7.7 \times 10^6 n_{e,7} \gamma_3^{-1} r_{\text{emi},10}^2 r_{c,10}^{-1} \text{ erg s}^{-1}$. Meanwhile, electrons will be accelerated by the rotating SS at the rate of $2\pi e B(r_{\text{emi}}) r_{\text{emi}} P_0^{-1} \sim 3.0 \times 10^3 r_6^3 r_{\text{emi},10}^{-2} B_{S,14} P_0^{-1} \text{ erg s}^{-1}$ (Kashiyama et al. (2013)), where $B(r_{\text{emi}})$ is the magnetic field strength at r_{emi} . The maximum Lorentz factor during coherent emission thus can be obtained, $\gamma_{\text{max}} \sim 2.6 \times 10^6 n_{e,7} r_{\text{emi},10}^4 r_{c,10}^{-1} r_6^3 B_{S,14}^{-1} P_0$, which is large enough for FRBs.

4. COUNTERPARTS IN OTHER WAVEBANDS

No counterparts of FRBs have been discovered in other wavebands yet, except for the repeating FRB, FRB 121102 (Michilli et al. (2018)). The collapse of a SS crust might result in electromagnetic radiation besides radio (Petroff et al. (2015)). It's intriguing to check whether the emissions in other wavebands is strong or not in our model.

There are mainly two types of emission from a bare SS surface, thermal radiation and e^+e^- pair emission (Usov (2001a)). The plasma frequency for an SQM object can be written as

$$\omega_p = \left(\frac{8\pi}{3} \frac{e^2 c^2 n_b}{\mu} \right)^{1/2}, \quad (7)$$

where n_b is the baryon number density of SQM and $\mu \simeq \hbar c (\pi^2 n_b)^{1/3}$ (Alcock et al. (1986)). According to the plasma dispersion relationship, propagating modes for electromagnetic waves with $\omega < \omega_p$ do not exist. For typical SQM $n_b \simeq (1.5 \sim 2)n_0$, where $n_0 \simeq 1.7 \times 10^{38} \text{ cm}^{-3}$ is normal nuclear matter density, we expect $\hbar \omega_p \simeq 20\text{--}25 \text{ MeV}$. Thus SSs with a surface temperature T_S below $2 \times 10^{10} \text{ K}$ are very poor radiators for blackbody radiation. However, the thermal radiation luminosity increases sharply and becomes the chief emission form if $T_S \geq 5 \times 10^{10} \text{ K}$ (Haensel & Zdunik (1991); Alcock et al. (1986)). The energy flux per unit surface in thermal photons is $F_{\text{eq}} = \frac{\hbar}{c^2} \int_{\omega_p}^{\infty} \frac{\omega(\omega^2 - \omega_p^2)g(\omega)}{\exp(\hbar\omega/k_B) - 1} d\omega$, where $g(\omega) = \frac{1}{2\pi^2} \int_0^{\pi/2} D(\omega, \theta) \sin \theta \cos \theta d\theta$, κ_B is the Boltzmann constant, $D(\omega, \theta)$ is the coefficient of radiation transmission from SQM to the vacuum, $D = 1 - (R_{\perp} + R_{\parallel})$, and $R_{\perp} = \sin^2(\theta - \theta_0)/\sin^2(\theta + \theta_0)$, $R_{\parallel} = \tan^2(\theta - \theta_0)/\tan^2(\theta + \theta_0)$, $\theta_0 = \arcsin[\sin \sqrt{1 - (\omega_p/\omega)^2}]$ (Usov (2001a)).

As pointed out by Usov (1998b), the Coulomb barrier outside the SS surface is a very powerful source of e^+e^- pairs, where the electronic field $\sim 5 \times 10^{17} \text{ V cm}^{-1}$ is tens of times higher than the critical vacuum polarization field $E_{\text{cr}} = m^2 c^3 / e \hbar \simeq 1.3 \times 10^{17} \text{ V cm}^{-1}$. e^+e^- pairs are created with the mean particle energy of $\varepsilon_{\pm} \simeq m_e c^2 + kT_S$. The flux of pairs is

$$f_{\pm} \simeq 10^{39.2} \left(\frac{T_S}{10^9 \text{ K}} \right) \exp \left(-\frac{11.9 \times 10^9 \text{ K}}{T_S} \right) J(\xi) \text{ s}^{-1}, \quad (8)$$

where

$$J(\xi) = \frac{1}{3} \frac{\xi^3 \ln(1 + 2\xi^{-1})}{(1 + 0.074\xi)^3} + \frac{\pi^5}{6} \frac{\xi^4}{(13.9 + \xi)^4}, \quad (9)$$

and $\xi \simeq (2 \times 10^{10} \text{ K})/T_S$ (Usov (2001a)). The energy flux per unit surface in e^+e^- pairs is $F_{\pm} \simeq \varepsilon_{\pm} f_{\pm}$.

Since the radiation features of a bare SS are determined by T_S , it is crucial to study the distribution of temperature and how it evolves. The heat transfer equation for SSs under the plane-parallel approximation is (Usov (2001b); Iwamoto (1982); Heiselberg & Pethick (1993))

$$C_q \frac{\partial T}{\partial t} = \frac{\partial}{\partial x} \left(K_c \frac{\partial T}{\partial x} \right) - \varepsilon_{\nu}, \quad (10)$$

where $C_q \simeq 2.5 \times 10^{20} (n_b/n_0)^{2/3} T_9 \text{ erg cm}^{-3} \text{ K}^{-1}$ is the specific heat for SQM per unit volume, $K_c \simeq 6 \times 10^{29} \alpha_c^{-1} (n_b/n_0)^{2/3} \text{ erg cm}^{-1} \text{ K}^{-1}$ is the thermal conductivity, $\varepsilon_{\nu} \simeq 2.2 \times 10^{26} \alpha_c Y_e^{1/3} (n_b/n_0) T_9^6 \text{ erg cm}^{-3} \text{ s}^{-1}$ is the neutrino emissivity, $n_b \sim 2n_0$ is the SQM baryon number density, $\alpha_c = g^2/4\pi \sim 0.1$ is the QCD fine structure constant with g being the quark-gluon coupling constant, and $Y_e = n_e/n_b \sim 10^{-4}$ is the number ratio between electrons and baryons. Due to thermal conductivity, the heat flux is

$$q = -K_c dT/dx. \quad (11)$$

The boundary condition is $q \simeq -F_{\pm} - F_{\text{eq}}$.

We now proceed to calculate the evolution of the radiation luminosity after the collapse of an SS crust. Our calculations are done for an SS with an initial surface and crust temperature of $T_{S0} \sim 3 \times 10^7 \text{ K}$ (Pizzochero (1991); Usov (1997)), and a crust mass of $M_c \sim 3 \times 10^{-6} M_{\odot}$. There are mainly two kinds of energy released during the collapse: (1) gravitational energy of the crust ($\sim 0.002 M_c c^2$) due to its radical movement to the SQM surface, and (2) deconfinement energy ($\sim 0.01 - 0.03 M_c c^2$) due to the conversion of the crust material to SQM (Cheng & Dai (1996)).

As a sum, we can take the typical total energy from these two reservoirs as roughly $Q \sim 0.02 M_c c^2 \sim 1 \times 10^{47}$ erg for $M_c \sim 3 \times 10^{-6} M_\odot$. After the collapse, the crust is transferred to SQM with a density of $\sim 5 \times 10^{14}$ g cm $^{-3}$ [Alcock et al. \(1986\)](#) and the interaction is restricted in a thickness of $l^* \sim 1$ cm. Assuming the actual combustion mode is detonation [Olinto \(1987\)](#); [Horvath & Benvenuto \(1988\)](#); [Heiselberg et al. \(1991\)](#), the timescale of conversion is rather small and the interior SS temperature can be treated as uninfluenced while the surface layer is hot and isothermal. With $C_q \sim 4 \times 10^{11}$ T erg cm $^{-3}$ K $^{-1}$, the temperature of the heated layer can be estimated as $T_S^* \sim 2 \times 10^{11}$ K. The initial temperature distribution can be expressed as

$$T(t=0, x) \simeq \begin{cases} T_S^*, & 0 < x < l^* \\ T_{S0}, & x \geq l^*, \end{cases} \quad (12)$$

where t is the time after the collapse and x is a space coordinate measuring the depth below the SS surface.

Combing these postulations and approximations, we have performed numerical calculations to solve the cooling process. Figure 2 shows the evolution of the surface temperature as a function of time. The total luminosity including both photons and electrons/positrons, $L = L_{\text{eq}} + L_\pm = 4\pi r^2 (F_{\text{eq}} + F_\pm)$, has also been calculated and the result is shown in Figure 3. We should note that when L_\pm is very high, most of the pairs will annihilate into photons near the SS surface due to the high pair density. Hence the emerging emission consists mostly of photons. The photon spectrum is roughly a blackbody with a high energy (> 100 keV) tail [Aksenov et al. \(2003\)](#) since the outgoing pairs and photons are very likely in thermal equilibrium [Iwamoto & Takahara \(2002\)](#). Note that bare SSs are bounded by strong interactions rather than the gravity, so the luminosity can safely exceed the Eddington limit [Alcock et al. \(1986\)](#).

The luminosity distance is $d_L \sim$ a few hundred Mpc at redshift of $z \sim 0.5 - 1$. The hot bare SS radiates at an extremely high luminosity just after the collapse and it cools down rapidly. The surface layer will become cold soon, making the radiation power decrease quickly. Since $T_S \sim$ a few 10^9 K during the emission, the typical photon energy can be estimated as ~ 100 keV for a blackbody spectrum. According to our calculations, the emitted energies are roughly 9.6×10^{44} erg, 1.6×10^{45} erg, and 1.7×10^{45} erg in the first 10 ms, 100 ms, and 1000 ms after the collapse, respectively. If averaged over 100 ms, the typical luminosity is $L \sim 2 \times 10^{46}$ erg s $^{-1}$. Noting that the expected radiation flux is then $10^{-8} L_{46} (d_L/100 \text{ Mpc})^{-2}$ erg cm $^{-2}$ s $^{-1}$, this luminosity will be too low to trigger Swift BAT, whose threshold is $\sim 10^{-7}$ erg cm 2 s $^{-1}$ in 15–150 keV [Lorén-Aguilar et al. \(2009\)](#). Also, the derived peak photon flux of $\sim 0.1 (d_L/100 \text{ Mpc})^{-2}$ photons cm $^{-2}$ s $^{-1}$ is lower than the trigger threshold of Fermi GBM, 0.74 photons cm $^{-2}$ s $^{-1}$ [Meegan et al. \(2009\)](#). Additionally, the extremely small radiation timescale of about 0.1 s makes the observation even more difficult. Although convection process may reheat the SS surface and increase its emission slightly [Usov \(1998a\)](#), the light curve within initial 0.1 s will not be influenced significantly and no afterglow could be detected in X-rays or gamma-rays by current high energy detectors.

5. SUMMARY AND DISCUSSION

In summary, we propose that FRBs may be generated from the collapses of strange star crusts. During the collapse, a fraction of magnetic energy is transferred to accelerate electrons and positrons in the polar cap region to relativistic velocities. The accelerated electrons expand along magnetic field lines to form a shell. At the radius of $r_{\text{emi}} \sim 10^{10}$ cm, coherent emission in radio bands will be produced, giving birth to the observed FRB. At the same time, the emission in X-ray and γ -ray bands is too faint to be detected by current detectors.

It is argued that the magnetic field of an SS is influenced by spacial temperature variations [Xu & Busse \(2001\)](#). The SQM surface will be heated up to a high temperature of $\sim 10^{11}$ K and cool down drastically via the production of electron-positron pairs and neutrinos [Usov \(1998b, 2001b\)](#). A thin layer surface will be even colder than inside during the cooling process. A cold dense layer forms and then the temperature distribution seems unstable with respect to convective disturbances [Usov \(1998a\)](#). The small-scale buoyant convection induced by temperature gradient may amplify the magnetic field due to the interaction with differential rotation through fast dynamos processes [Xu & Busse \(2001\)](#). The amplified magnetic field lines may emerge from the stellar interior, where the fields can be several order-of-magnitude larger [Shibata & Magara \(2011\)](#). A fraction of heat may be transferred to magnetic field energy and then also contribute to the emission. In other words, the SS surface magnetic field strength may increase significantly after the collapse, thus SSs originally having a weaker magnetic field may also produce FRBs. The effect of convection needs further investigation in the future.

It is an interesting question whether FRBs generated from SS crust collapses can repeat or not. The crux is to determine whether a bare SS can re-construct its crust through accretion or other ways. In fact, most SS formation models are explosive [Haensel et al. \(1991\)](#); [Xu et al. \(2001\)](#); [Pagliara et al. \(2013\)](#), thus a newly-born SS is bare and

how a normal matter crust forms still needs to be investigated. The free-fall kinetic energy for a proton onto SS surface is $E_p \simeq \frac{GMm_p}{R\sqrt{1-2GM/Rc^2}} \approx 138 M_1 R_6^{-1} (1 + 0.2 M_1 R_6^{-1}) \text{ MeV}$ [Olinto \(1987\)](#), where m_p is the proton mass. If the SS is non-rotational and not magnetized, and the accretion is isotropic, then the free-fall energy will be high enough to overcome the electrostatic potential barrier of $eV \simeq 20 \text{ MeV}$ outside the SQM surface [Alcock et al. \(1986\)](#). So, SS crusts cannot be built in such scenarios. However, the falling material will have a non-zero angular momentum when approaching the surface of rotational magnetized SSs due to the magnetic freezing. These matter will finally hit the SS surface obliquely at a typical incidence angle with cotangent ~ 0.05 [Olinto \(1987\)](#); [Kluźniak & Wagoner \(1985\)](#). Hence the accreted matter has a longer interaction with the electric field and the radial velocity will be reduced by friction and radiation. Considering this effect, an envelope built from the accreted material will cover the whole SQM core gradually. If the accretion continues, the crust will finally reach the critical mass via accretion and then collapse.

In this case, the number density of particles near the SS may be rather high due to the existence of the accretion flow. Thus the interaction between the expanding shell and the accretion flow needs to be considered. Assuming that the accretion is isotropic, the number density of the accretion flow at the emission radius is $n_a \approx 2\dot{M} / [4\pi r_{\text{emi}}^2 m_p (2GM/r_{\text{emi}})^{1/2}] \sim 1.6 \times 10^5 (\dot{M}/10^{-15} M_\odot \text{ yr}^{-1}) (M/1.4 M_\odot) r_{\text{emi},10}^{-3/2} \text{ cm}^{-3}$, where \dot{M} is the accretion rate. If the accreting rate is high, the outgoing shell may be disrupted by the falling gas and then no FRB could be generated. However, as long as \dot{M} is less than a critical value of $\dot{M}_{\text{cr}} \approx 10^{-15} M_\odot \text{ yr}^{-1}$, we notice that n_a will be much smaller than the number density of electrons in the expanding shell (n_e). Then the influence of the accretion flow can be negligible.

For SSs formed in explosive events [Haensel et al. \(1991\)](#); [Xu et al. \(2001\)](#); [Pagliara et al. \(2013\)](#), the compact stars may receive a “kick” if these drastic events are asymmetric [Nordhaus et al. \(2012\)](#); [Bray & Eldridge \(2016\)](#). The typical kick velocity, v , ranges from 200 to 400 km s^{-1} , with the highest value even in excess of 1000 km s^{-1} [Lyne & Lorimer \(1994\)](#); [Faucher-Giguère & Kaspi \(2006\)](#). SSs with a kick velocity would accrete ambient matter at a rate of $\dot{M} \approx 2\pi\alpha(GM)^2 v^{-3} \rho \sim 2 \times 10^{-15} M_1^2 \rho_{-21} v_7^{-3} M_\odot \text{ yr}^{-1}$, where $\alpha \sim 1.25$ is a numerical constant and ρ is the ambient matter density [Bondi \(1952\)](#). In this case, the typical \dot{M} would not exceed \dot{M}_{cr} significantly. Therefore, the expanding electron/positron shell can expand without being destroyed by the accretion flow in our scenario. For this kind of accretion, the reconstruction timescale of the crust can be roughly estimated as $\tau_{\text{rec}} \approx M_c / \dot{M}_{\text{cr}} \sim 10^9 \text{ yr}$.

Owing to this long reconstruction timescale, multiple FRB events from the same source seem not likely to happen in our scenario. Our model thus is more suitable for explaining the non-repeating FRBs, and the repeating FRB 121102 may be produced via other mechanisms [Palaniswamy et al. \(2018\)](#). However, we should also note that during the collapse process, if only a small portion (in the polar cap region) of the crust falls onto the SQM core while the other portion of the crust remains stable, then the rebuilt timescale for the crust can be markedly reduced and repeating FRBs would still be possible. Further detailed studies on the crust collapse thus still need to be conducted.

The event rate of FRBs is as high as $2 \times 10^3 \text{ sky}^{-1} \text{ day}^{-1}$ [Bhandari et al. \(2018\)](#); [Li et al. \(2017\)](#). There are roughly $\sim 10^9$ galaxies within the redshift range of $z \leq 1$ and the total number of pulsars per galaxy is $\sim 10^8$ on average [Timmes et al. \(1996\)](#). The event rate for SS crust collapse can be estimated as $\sim 2 \times 10^3 (\tau_{\text{rec}}/10^9 \text{ yr})^{-1} f f_{\text{S},-3}$, where f is the beaming factor of radio emission, and f_{S} is the number ratio of SSs with compatible conditions to generate FRBs over pulsars. Still, we would like to remind that FRBs may be of multiple origin and our model may only contribute a portion of them. Further observations and larger samples in the future would help to solve the enigma finally.

We appreciate valuable comments and constructive suggestions from the anonymous referee. This work is supported by the National Natural Science Foundation of China (Grant No. 11473012), the National Basic Research Program (“973” Program) of China (Grant No. 2014CB845800), the National Postdoctoral Program for Innovative Talents (Grant No. BX201700115), the China Postdoctoral Science Foundation funded project (Grant No. 2017M620199), and the Strategic Priority Research Program “Multi-waveband gravitational wave Universe” (Grant No. XDB23040000) of the Chinese Academy of Sciences.

REFERENCES

- | | |
|--|---|
| <p>Abe, K., Bacon, T. C., Ballam, J., et al. 1984, <i>PhRvD</i>, 30, 1</p> <p>Aksenov, A. G., Milgrom, M., & Usov, V. V. 2003, <i>MNRAS</i>, 343, L69</p> <p>Alcock, C., Farhi, E., & Olinto, A. 1986, <i>ApJ</i>, 310, 261</p> <p>Barrau, A., Rovelli, C., & Vidotto, F. 2014, <i>PhRvD</i>, 90, 127503</p> | <p>Benford, G., & Buschauer, R. 1977, <i>MNRAS</i>, 179, 189</p> <p>Bhandari, S., Keane, E. F., Barr, E. D., et al. 2018, <i>MNRAS</i>, 475, 1427</p> <p>Bondi, H. 1952, <i>MNRAS</i>, 112, 195</p> <p>Bray, J. C., & Eldridge, J. J. 2016, <i>MNRAS</i>, 461, 3747</p> |
|--|---|

- Cheng, K. S., & Dai, Z. G. 1996, *Physical Review Letters*, 77, 1210
- Chmaj, T., Haensel, P., & Słomiński, W. 1991, *Nuclear Physics B Proceedings Supplements*, 24, 40
- Cordes, J. M., & Lazio, T. J. W. 2002, arXiv:astro-ph/0207156
- Dai, Z. G., Wang, J. S., Wu, X. F., & Huang, Y. F. 2016, *ApJ*, 829, 27
- Falcke, H., & Rezzolla, L. 2014, *A&A*, 562, A137
- Farhi, E., & Jaffe, R. L. 1984, *PhRvD*, 30, 2379
- Faucher-Giguère, C.-A., & Kaspi, V. M. 2006, *ApJ*, 643, 332
- Geng, J. J., & Huang, Y. F. 2015, *ApJ*, 809, 24
- Geng, J. J., Huang, Y. F., & Lu, T. 2015, *ApJ*, 804, 21
- Gu, W.-M., Dong, Y.-Z., Liu, T., Ma, R., & Wang, J. 2016, *ApJL*, 823, L28
- Haensel, P., Paczynski, B., & Amsterdamski, P. 1991, *ApJ*, 375, 209
- Haensel, P., Zdunik, J. L., & Schaefer, R. 1986, *A&A*, 160, 121
- Haensel, P. 1991, *Nuclear Physics B Proceedings Supplements*, 24, 23
- Haensel, P., & Zdunik, J. L. 1991, *Nuclear Physics B Proceedings Supplements*, 24, 139
- Heiselberg, H., Baym, G., & Pethick, C. J. 1991, *Nuclear Physics B Proceedings Supplements*, 24, 144
- Heiselberg, H., & Pethick, C. J. 1993, *PhRvD*, 48, 2916
- Horvath, J. E., & Benvenuto, O. G. 1988, *Physics Letters B*, 213, 516
- Huang, Y. F., & Lu, T. 1997, *A&A*, 325, 189
- Iwamoto, N. 1982, *Annals of Physics*, 141, 1
- Iwamoto, S., & Takahara, F. 2002, *ApJ*, 565, 163
- Kashiyama, K., Ioka, K., & Mészáros, P. 2013, *ApJL*, 776, L39
- Katz, J. I. 2014, *PhRvD*, 89, 103009
- Keane, E. F., Stappers, B. W., Kramer, M., & Lyne, A. G. 2012, *MNRAS*, 425, L71
- Kettner, C., Weber, F., Weigel, M. K., & Glendinning, N. K. 1995, *PhRvD*, 51, 1440
- Kluźniak, W., & Wagoner, R. V. 1985, *ApJ*, 297, 548
- Kondratyuk, L. A., Krivoruchenko, M. I., & Martemyanov, B. V. 1990, *Soviet Astronomy Letters*, 16, 410
- Kouveliotou, C., Dieters, S., Strohmayer, T., et al. 1998, *Nature*, 393, 235
- Kulkarni, S. R., Ofek, E. O., Neill, J. D., Zheng, Z., & Juric, M. 2014, *ApJ*, 797, 70
- Kumar, P., Lu, W., & Bhattacharya, M. 2017, *MNRAS*, 468, 2726
- Lai, D., & Shapiro, S. L. 1991, *ApJ*, 383, 745
- Lai, X.-Y., Yu, Y.-W., Zhou, E.-P., Li, Y.-Y., & Xu, R.-X. 2018, *Research in Astronomy and Astrophysics*, 18, 024
- Lattimer, J. M., & Prakash, M. 2007, *PhR*, 442, 109
- Li, L.-B., Huang, Y.-F., Zhang, Z.-B., Li, D., & Li, B. 2017, *Research in Astronomy and Astrophysics*, 17, 6
- Liu, X. 2017, arXiv:1712.03509
- Lorén-Aguilar, P., Isern, J., & García-Berro, E. 2009, *A&A*, 500, 1193
- Lorimer, D. R., Bailes, M., McLaughlin, M. A., Narkevic, D. J., & Crawford, F. 2007, *Science*, 318, 777
- Luan, J., & Goldreich, P. 2014, *ApJL*, 785, L26
- Lyne, A. G., & Lorimer, D. R. 1994, *Nature*, 369, 127
- Lyubarsky, Y. 2008, *ApJ*, 682, 1443-1449
- Meegan, C., Lichti, G., Bhat, P. N., et al. 2009, *ApJ*, 702, 791-804
- Melrose, D. B. 1971, *Ap&SS*, 13, 56
- Michilli, D., Seymour, A., Hessels, J. W. T., et al. 2018, *Nature*, 553, 182
- Miralda-Escude, J., Paczynski, B., & Haensel, P. 1990, *ApJ*, 362, 572
- Nordhaus, J., Brandt, T. D., Burrows, A., & Almgren, A. 2012, *MNRAS*, 423, 1805
- Olinto, A. V. 1987, *Physics Letters B*, 192, 71
- Pagliara, G., Herzog, M., & Röpkke, F. K. 2013, *PhRvD*, 87, 103007
- Palaniswamy, D., Li, Y., & Zhang, B. 2018, *ApJL*, 854, L12
- Petroff, E., Bailes, M., Barr, E. D., et al. 2015, *MNRAS*, 447, 246
- Pizzochero, P. M. 1991, *Physical Review Letters*, 66, 2425
- Rees, M. J., & Mészáros, P. 1992, *MNRAS*, 258, 41P
- Romero, G. E., del Valle, M. V., & Vieyro, F. L. 2016, *PhRvD*, 93, 023001
- Ruderman, M. A., & Sutherland, P. G. 1975, *ApJ*, 196, 51
- Scholz, P., Spitler, L. G., Hessels, J. W. T., et al. 2016, *ApJ*, 833, 177
- Shibata, K., & Magara, T. 2011, *Living Reviews in Solar Physics*, 8, 6
- Spitler, L. G., Scholz, P., Hessels, J. W. T., et al. 2016, *Nature*, 531, 202
- Stejner, M., & Madsen, J. 2005, *PhRvD*, 72, 123005
- Thompson, C., & Duncan, R. C. 1995, *MNRAS*, 275, 255
- Thornton, D., Stappers, B., Bailes, M., et al. 2013, *Science*, 341, 53
- Timmes, F. X., Woosley, S. E., & Weaver, T. A. 1996, *ApJ*, 457, 834
- Totani, T. 2013, *PASJ*, 65, L12
- Usov, V. V. 1997, *ApJL*, 481, L107
- Usov, V. V. 1998a, *Physical Review Letters*, 81, 4775
- Usov, V. V. 1998b, *Physical Review Letters*, 80, 230
- Usov, V. V. 2001a, *ApJL*, 550, L179
- Usov, V. V. 2001b, *Physical Review Letters*, 87, 021101
- Wang, W., Luo, R., Yue, H., et al. 2018, *ApJ*, 852, 140
- Witten, E. 1984, *PhRvD*, 30, 272
- Xu, R. X., & Busse, F. H. 2001, *A&A*, 371, 963
- Xu, R. X., Zhang, B., & Qiao, G. J. 2001, *Astroparticle Physics*, 15, 101
- Zhang, B. 2014, *ApJL*, 780, L21

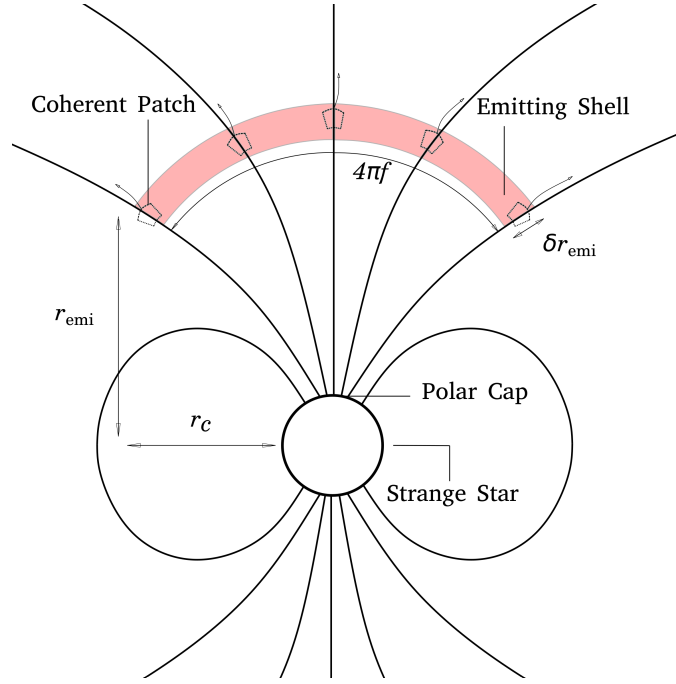


Figure 1. A schematic illustration of how an FRB is generated after the collapse of the strange star crust. Electrons are accelerated to relativistic velocities and expand along the magnetic field lines to form a shell. Coherent emission at radio wavelength is produced when the shell radius reaches r_{emi} .

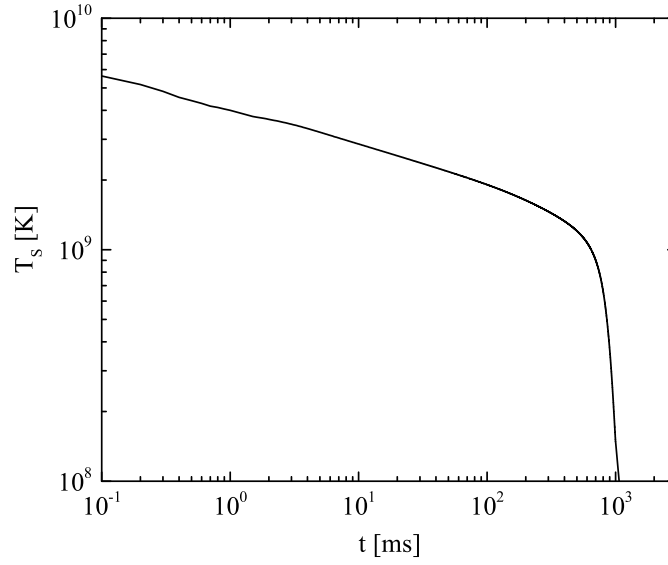


Figure 2. Evolution of the surface temperature of a bare strange star, T_{S} , after the crust collapses.

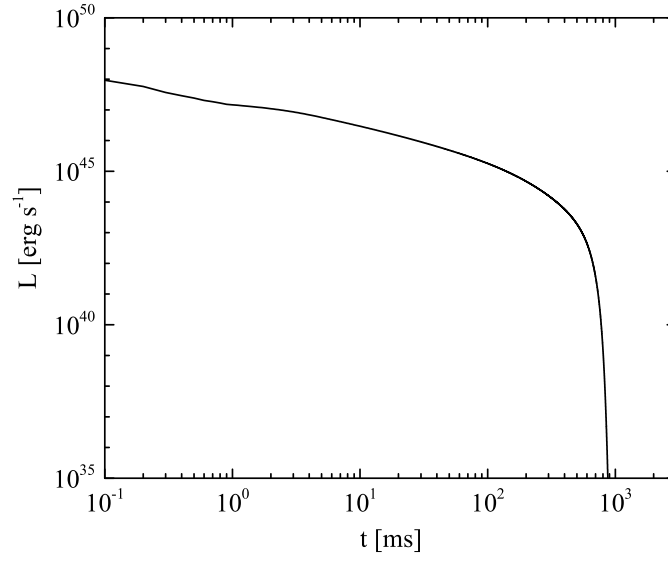


Figure 3. Total luminosity, L , as a function of time after the crust collapses. In this figure, $L = L_{\pm} + L_{\text{eq}}$, where L_{\pm} and L_{eq} are the luminosities in thermal photons and e^+e^- pairs, respectively.